

# From Demonstration to Operation: High Contrast Imaging Tools at Keck Observatory

Charlotte E. Guthery<sup>1</sup>, Jacques Delorme<sup>1</sup>, Michael Bottom<sup>2</sup>, Sam Walker<sup>3</sup>, Maria Vincent<sup>3</sup>, Rebecca Jensen-Clem<sup>4</sup>, Maïssa Salama<sup>4</sup>, Vincent Chambouleyron<sup>4</sup>, Jules Fowler<sup>4</sup>, Maaike van Kooten<sup>5</sup>, J. Kent Wallace<sup>6</sup>, Charlotte Z. Bond<sup>7</sup>, Sylvain Cetre<sup>8, 9</sup>, Sam Ragland<sup>1</sup>, and Peter Wizinowich<sup>1</sup>

<sup>1</sup>W. M. Keck Observatory, 65-1120 Mamalahoa Hwy. Kamuela, HI 96743 USA
<sup>2</sup>Institute for Astronomy, 640 North A'ohōkū Pl. Hilo, HI 96720-2700 USA
<sup>3</sup>Institute for Astronomy, 2680 Woodlawn Dr. Honolulu, HI 96822 USA
<sup>4</sup>University of California Santa Cruz, 1156 High St. Santa Cruz, CA 95064 USA
<sup>5</sup>Herzberg Astronomy and Astrophysics Research Centre, 5071 West Saanich Rd. Victoria, British Columbia
<sup>6</sup>Jet Propulsion Laboratory, California Institute of Technology, 4800 Oak Grove Dr. Pasadena, CA 91109 USA
<sup>7</sup>The UK Astronomy Technology Centre, Royal Observatory Edinburgh, Edinburgh, UK
<sup>8</sup>Durham University, Stockton Road, Durham, UK
<sup>9</sup>Wakea Consulting, Grenoble, Auvergne-Rhône-Alpes, France

### ABSTRACT

High contrast imaging (HCI) is limited in practice by uncorrected wavefront errors within traditional adaptive optics (AO). Keck observatory experiences roughly 130nm of unacoounted residual wavefront error even with well calibrated AO [15]. Multiple HCI tools currently in development are presented, focused on minimizing these errors and improving contrast during typical observation nights: (1) Fast and Furious is a focal plane wavefront sensing algorithm shown to correct for large portions of non-common path aberrations between the NIRC2 science instrument and the primary Keck wavefront sensor (WFS) [1]. On sky demonstrations of an operational version of this algorithm show an increase in Strehl ratio up to 19% in a single run. (2) The Keck primary mirror phasing is known to degrade between routine segment exchanges [14]. A Zernike wavefront sensor (ZWFS) is currently installed within the Keck Planet Imager and Characterizer (KPIC) to take passive measurements of the primary mirror to maintain the phasing. The detection of segment piston wavefront errors down to 50 nm with the ZWFS demonstrates the first step of maintaining phasing in parallel with science observations [11]. (3) Operational speckle nulling algorithms are in test to minimize bright speckles during HCI [2]. (4) As an addition to an upgraded real time controller, predictive wavefront control will be further developed to minimize errors due to large windspeeds and servo lag [12]. These HCI demonstrations will be built as reliable, robust, and simple to control operational tools which will become available to greatly benefit observers.

**Keywords:** Adaptive Optics, High Contrast Imaging, Wavefront Sensing

Further information: cguthery@keck.hawaii.edu

#### 1. INTRODUCTION TO BUILDING OPERATIONAL TOOLS

Many HCI imaging projects at Keck observatory have been demonstrated in a lab setting or minimally on-sky with positive results. One barrier to advance these projects is that they require experts to run and often only those who developed the tool have knowledge on operating them. This greatly limits the application of these projects on science observations. Building operational tools which are easy to use and robust on sky will increase the application of these projects and their benefit for the observatory. Transitioning HCI projects from a demonstration phase to an operational tool requires several changes to the software, interface, and accessibility to overcome these obstacles.

#### 1.1 Determining Feasibility

Building an operational tool will always take additional time and effort past the initial demonstration. Before committing time and resources to this effort, it is important to decide whether a transition to operation is even viable for a specific project. A balance must be reached between the time and money it takes to build the tool and the benefit for observers. This process begins by answering the following questions.

- 1. **Do observers want this?** Science observers are the intended beneficiaries of HCI tools. If the observers are uninterested in the results, or if the tool does not solve a problem they are effected by, it would have little motivation to be run. At this stage of the project, the user should clearly define the science applications this tool would be used for. Knowing the observers who would benefit from this upgrade is an important factor for this transition.
- 2. How much time will it take to build? Any transition of a project will take effort from the observatory and the demonstration group. A clear picture of these hours will inform the plans for building the tool. If the tool requires permanent hardware to be added, more hours and manpower will be needed.
- 3. How will this impact normal scientific observations? Deciding how a project is run during an observation night is important to understand how it may impact normal operations. If a project will take time away from science to run, it may need to show a more substantial improvement than one which can run in parallel. It should be expected that the tool may fault at some stage, especially when first integrating it into operations. The effects of this fault should be well known; can the operation be reverted easily or will science observations lose time on sky?

Whether a project is chosen for an operational tool depends on the answers to all three questions. A tool which requires very little effort to build and does not interfere with normal observations would only need to show minimal improvements to science to be approved. However, a tool requiring dedicated time and hardware to build would need to show substantial changes, solving some problem faced by many observers. Balancing this information can determine whether a tool should be fully transitioned into operations, a process explained in Section 1.2.

#### 1.2 Steps for Transitioning to Operations

- 1. Evaluate the current status. The development team must be fully aware of how the project is currently operated. The first step is knowing how the project is connected to the current system hardware, such as cameras and deformation mirrors. Changes to the facility, software or hardware, must be known. Documentation or instructions to train operators need to be consolidated and read through.
- 2. **Develop the first graphic user interface (GUI) control.** The first design focuses on translating all of the current controls to a GUI. The project should be fully operational through the GUI, with no need to access the source code.
- 3. Characterize on sky operation for different science targets. Operating the tool on multiple targets, AO configurations, elevations, and operation conditions will build a better understanding of expected performance. This will show if there are limits to operation such as target type, seeing conditions, guide star magnitudes, angle modes, or imaging parameters. This supports the development of a full understanding of the operation requirements for the tool.

- 4. **Iterate on the GUI design.** Updates to the GUI from Step 2 focus on simplifying the operation. This step should be iterative, the design updated whenever new control is needed. The goal for the final GUI is to minimize all unnecessary user inputs. The controls should be automated as much as possible to limit user errors.
- 5. Test robustness by attempting to fault the tool on sky. Finding the limits of the tool on sky helps inform any necessary updates to the GUI or documentation. Letting a user with no experience run the tool is a good way to find missing instructions or bugs in operation. This process is iterative and will make sure the tool is robust and easy to use once operational.
- 6. **Determine the desired operator.** The standard operator of the tool will inform the final design of the GUI as well as the documentation needed. If the operator does not need experience with AO, the documentation will need to account for that. If the operator is not an observatory employee additional instructions may need to be include to describe how to set up the tool.
- 7. **Develop appropriate documentation.** All information about the tool should be compiled in documentation. This includes how the tool is operated, who operates it, instructions for nightly setup, debugging, contact information for more complex errors, instructions to revert to normal operation. These details should be located in an easy to find place, so users can refer throughout the night.
- 8. Transfer the tool, GUI, and modules to an operations server. At this point, the tool and GUI design are presented to an operations team. That group must approve of the final design and deliverable for the tool's release. The final documentation must be approved and integration with the current operations software completed.
- 9. **Train the operators.** Once the tool is release the main operators are trained to run the tool. This process will inform any additional documentation on debugging efforts needed before a full release.

At the end of this process a previously demonstrated tool will be fully transitioned into an operational mode. The final deliverable includes backend software, user interface, and documentation.

# 2. FAST AND FURIOUS WAVEFRONT SENSING ALGORITHM

Fast and Furious (F&F) is a wavefront sensing and control algorithm used to improve PSF quality during the night with limited interference with observations. This algorithm uses science camera PSF images, as well as the previously applied DM correction to estimate slowly varying wavefront aberrations in the focal plane. More common focal plane wavefront sensing techniques generally require phase diversity, measuring defocused PSFs to break the sign paradox of even modes. F&F instead uses the previous DM correction and WFS estimate [10], as shown in Figure 4. The correction is then applied as centroid offsets with the Shack-Hartmann WFS (SHWFS) or slope changes with the PyWFS.

There are multiple benefits of using F&F over a more common image sharpening algorithm, such as Gerchberg Saxton or an additional WFS. 1) F&F requires no additional hardware, it only requires a connection with the science camera and AO system. 2) No calibration or diversity frames are needed, F&F can be run concurrently with science observations. 3) F&F works with narrow and broadband filters and bright or faint stars, so long as the PSF is well exposed on the science camera. 4) All aberrations in the optical system can be sensed and corrected, because F&F uses the science camera as the wavefront sensor. This includes non-common path aberrations (NCPAs), segment phasing errors, and the low wind effect. 5) F&F converges within 30 iterations, usually limited by detector readout and integration time. All of these benefits motivated an operational version of F&F to be deployed on the Keck telescopes.

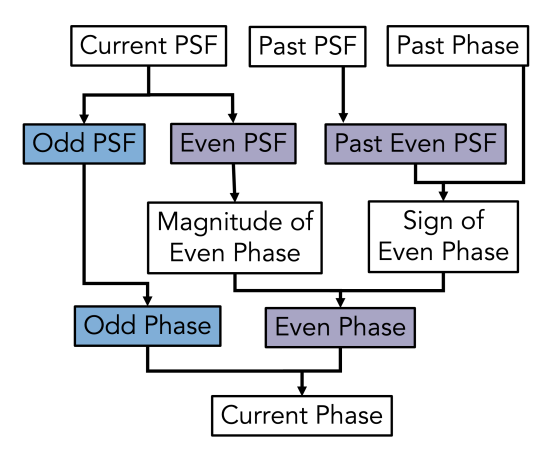


Figure 1. Shown is a flow chart which demonstrates how F&F uses the current focal plane image to directly solve for the odd component of the phase, and the magnitude of the even component. To solve for the sign of the even component, the previous focal plane image and corresponding DM correction is used.

#### 2.1 Characterization on Sky

The third step of transitioning a demonstrated project into an operation tool is to full characterize its response on-sky with fixed pupil mode. This is the simplest method of operation, using a star as the science object [1]. This is the simplest method of operations, with the main goal to get good wavefront correction on sky. The goals of these tests are the following 1) Determine how F&F should be run during a night 2) Characterize the response for a variety of science targets and NIRC2 set ups. It is important to note that the basic mode of F&F requires the science object to be a single star. 3) Test the stability of the tool. How often does it improve or degrade performance? Test how to revert the changes made?

One of the first operational notes about F&F is the limited performance in poor seeing conditions. F&F relies on some stability of the PSF between exposures to correct for NCPAs, as opposed to residual atmospheric errors. If the PSF shape drastically changes between iterations, F&F will not converge.

There is some flexibility with how F&F can be run throughout a night because it requires no diversity frames. It is possible to run F&F in parallel with science observations, by running an iteration whenever an observer triggers a new image, and constantly updating centroid offsets on the wavefront sensor. During the first half of the night on January 9th, 2023 F&F was rerun periodically to test its correction over time. The tests which show the largest improvement always occur when correcting the WFS offsets calculated during the day, there is much less improvement when running on top of already computed F&F offsets. The daytime calibrations are run with a light source internal to the Keck II AO bench, missing aberrations unseen by the WFS such as cophasing errors in the primary mirror. There were still improvements throughout the night, but they were minimal in comparison. This led to the conclusion that F&F should be run once at the beginning of the night, or after moving to a new science target.

During the same night, F&F was characterized for multiple targets and NIRC2 configurations. Multiple stars were tested ranging from an R-band magnitude of 6.7 to 11.6 with similar Strehl ratio improvements on each target. Additionally, multiple NIRC2 filters were tested with little change in performance. Shown in Figure 2 is the star 40 UMa, a magnitude 6.42 star imaged in K-band, when compared with the daytime calibrations F&F improved performance by 17%. Figure 3 shows an F&F run on the star BD+43 2140, a magnitude 7.37 star imaged in H-band, improving the Strehl ratio by 19%.

Nights used to characterize F&F performance on-sky used the base operation mode. To prioritize the release of this tool operations limits have been put in please to keep it reliable, while upgrades described in Section 2.3 are in progress. This mode runs with NIRC2, a diffraction limited facility class science instrument, during a natural guide star (NGS) AO observation with the Shack-Hartmann WFS (SHWFS).

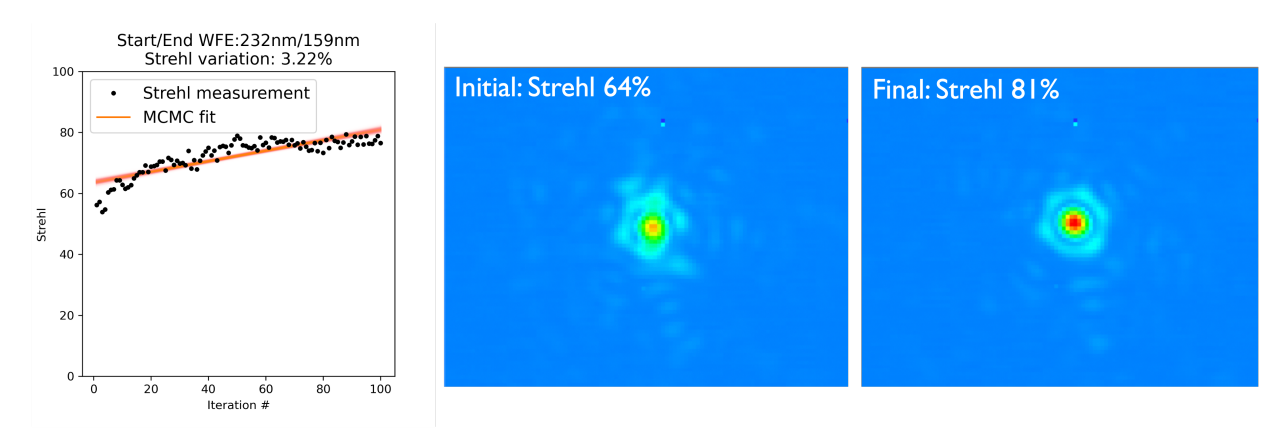


Figure 2. Results from testing F&F on January 9th, 2023. 40 UMa (K-band magnitude 6.42) imaged on NIRC2 with a bracket-gamma filter (K-band). Left displays the Strehl ratio changes for each iteration. Center is the NIRC2 image using typical daytime calibrations. Right is after F&F is run with 100 iterations (around 30 minutes) with a Strehl ratio improvement of 17%.

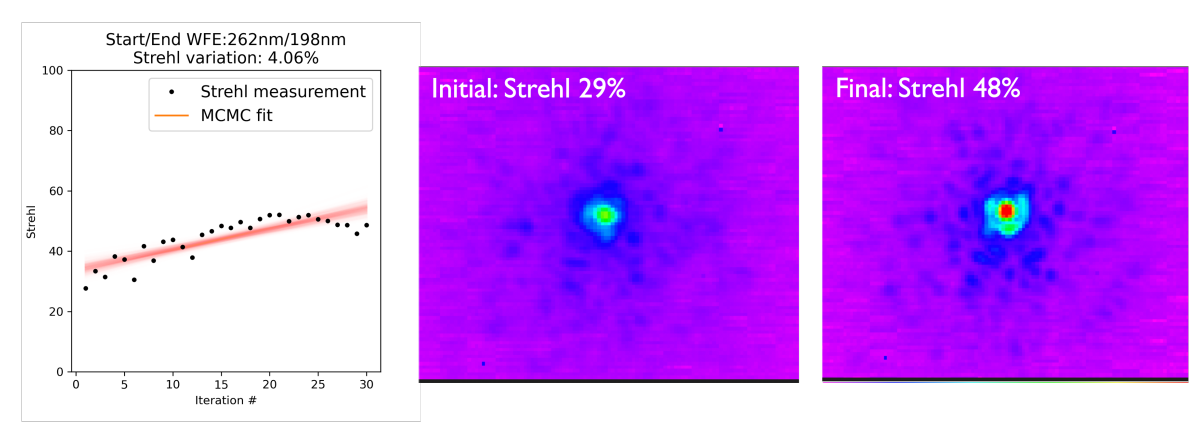


Figure 3. Results from testing F&F on January 9th, 2023. BD+43 2140 (H-band magnitude 7.37) imaged on NIRC2 with a ch4 short filter (H-band). Left is the NIRC2 image using typical daytime calibrations. Right is after F&F is run with 30 iterations (around 10 minutes) with a Strehl ratio improvement of 19%.

# 2.2 Operation Tool Design

The first step towards building F&F into an operational tool requires a restructuring of the algorithm control code. This change needs to minimize effects this tool may experience on normal nighttime observations, F&F must seamlessly integrate into normal telescope operations. One of the largest changes was logging telemetry data and WFS changes every time F&F updates AO software. The structure of how the F&F operation tool interacts with the WFS and Science instrument is shown in Figure 4.

While the algorithm runs, F&F will communicate with three different hardware components: the imaging sensor, deformable mirror, and wavefront sensor. In its most basic mode F&F is run using NIRC2 on the Keck II telescope with the SHWFS. When the algorithm begins it pulls all the current values set on NIRC2, including the current filter, pupil mask, integration time. F&F will trigger an exposure on NIRC2, the focal plane image in Figure 4. For the first iteration F&F uses a default phase error estimate of zero, all future iterations use the previous phase shape estimation for this component. With these values, the algorithm calculates centroid offsets representing the estimated residual phase error and applied them to the SHWFS. These offsets trigger the SHWFS to sense additional phase errors and correct for them with the DM. For each iteration the Strehl ratio on NIRC2 is monitored and the updated centroid offsets are recorded for record keeping.

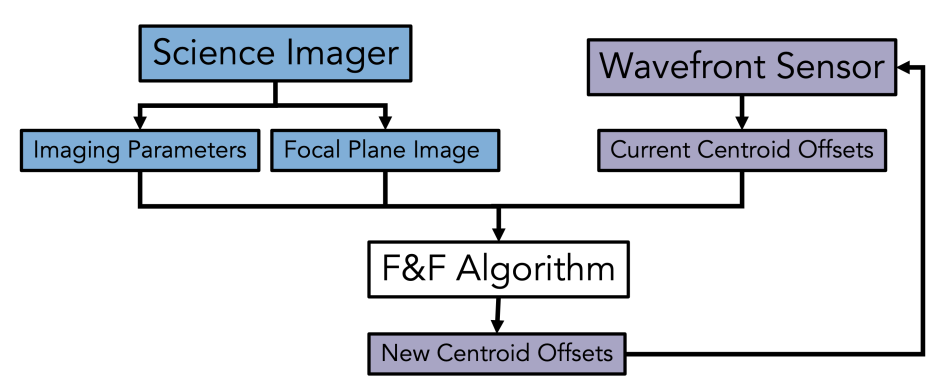


Figure 4. Schematic illustrating the connection between the F&F algorithm and software control of components (usually NIRC2 and the SHWFS).

The design of the user interface focuses the ease of use and accessibility of the tool. For F&F in particular, a simple GUI will allow the users to easily run the algorithm and update centroid offsets without any knowledge of the functions computing in the background. One of the ways to increase the accessibility, as well as the reliability with new users, is to minimize the necessary inputs for a user. For this reason the GUI is designed with the fewest inputs and buttons possible, automating as many functions as it can.

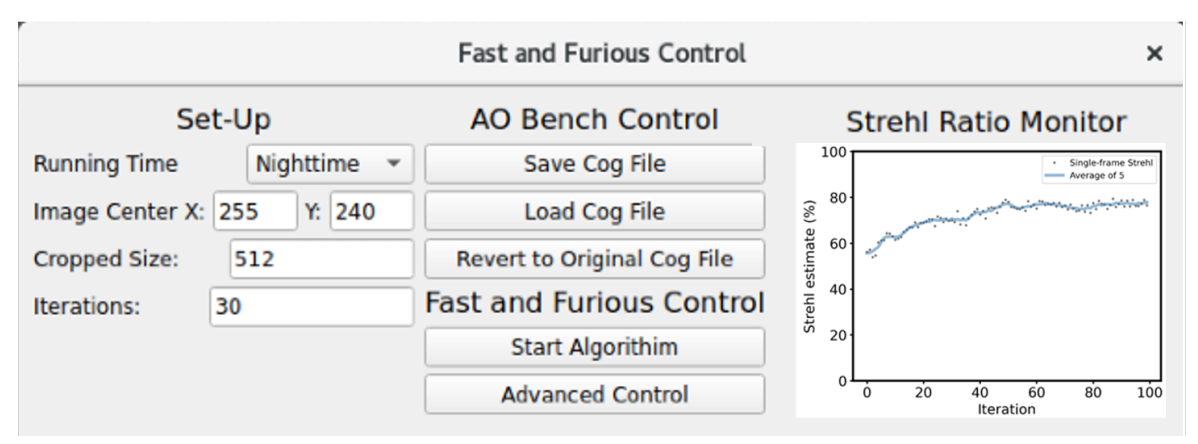


Figure 5. Current F&F GUI design to control the algorithm on-sky during a typical observation. The controls are limited to simplify operation, but an advanced control option allows users to change any input variables to the algorithm.

As seen in Figure 5, the operational tool requests only a few simple inputs from the observer. The center of the PSF on NIRC2 helps the algorithm crop around a region of interest. The number of iterations has suggested values in place, but can be changed to optimize performance. The rest of the controls are buttons allowing the user to load or save specific centroid offset (cog) files. The "Revert to Original Cog File" is important to maintain reliability of the AO system as a whole. For a worst case scenario, the user can easily restore the AO system to it's original configuration. The final buttons are used to start the algorithm or to open a much more detailed GUI for debugging more complex issues. This Advanced Control tool is only meant to be used for engineering. Altogether this tool has been designed to simplify operation of F&F such that observers can easily run the algorithm and improve their science on sky.

# 2.3 Final Tool and Planned Updates

F&F is scheduled to be released as an operational tool available for observers following the realtime controller upgrade on Keck II in November 2023. The released mode will only include the basic operation as described in Section 2.1. More advanced operational modes have been tests on-sky with promising results.

The basic mode of F&F runs with NGS AO, however on June 6th, 2023 F&F was tested during a laser guide star (LGS) science observation. This test was run to determine how F&F could operate with the additional complexities of LGS. The main concern was interfering with the low-bandwidth WFS (LBWFS), which corrects WFS centroid errors due to sodium layer variations. For this night the LBWFS was running with limited capacity, only correcting for focus errors. When run F&F showed a Strehl ratio improvement of 13%, shown in Figure 6.

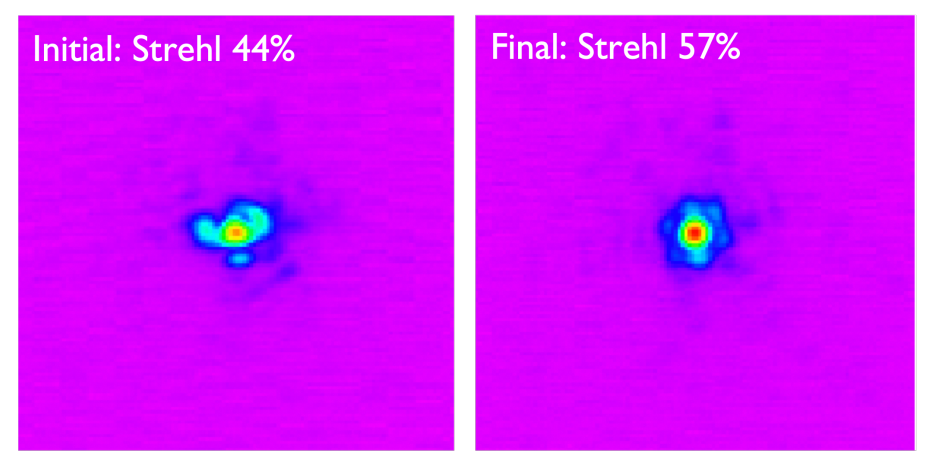


Figure 6. Results from testing F&F on June 6th, 2023 during a science observation with LGS. Shown are the before and after results from running F&F.

In addition to a LGS mode, there are multiple upgrades planned for the operational version of F&F. One of the main efforts will be to make it compatible with every AO-fed science instrument. Currently this would include OSIRIS on Keck I as well as KPIC on Keck II. Using F&F consistently for science on these instruments will motivate building functionality for future instruments such as HISPEC and SCALES. The Keck II telescope has the option of using the SHWFS or an IR pyramid WFS. F&F has run with the PyWFS successfully in the past, but this additional functionality will be included in a future upgrade. Currently F&F works with pupil tracking mode. A future upgrade will for on adapting the current algorithm to account for a fixed field PSF and rotating pupil instead. Finally, there is motivation to run F&F with Galactic Center observations. This will require upgrades to the algorithm itself to account for crowded field images instead of a single star. In all, these future upgrades will help adapt F&F into an easy to use operational tool to improve observations for most AO observations.

#### 3. PRIMARY MIRROR PHASING WITH A ZERNIKE WAVEFRONT SENSOR

Primary mirror segment cophasing errors are a contribute roughly 120nm to AO residual errors on both Keck telescopes. These errors must be corrected for the next generation of space and ground-based ELTs, which will

use segmented primary mirrors. A ZWFS is ideal for differentiating cophasing errors from other AO residuals, due to the fact that it directly images the pupil plane as a type of interferometer. The ZWFS consists of a focal plane mask to impose a phase offset to the very core of the PSF. The core interferes with the remaining PSF light to convert phase variations to intensity changes visible in the pupil image.

The ZWFS is located in the imaging path of the KPIC instrument [9]. The collimated light entering the KPIC instrument passes through a filter wheel before being focused on the ZWFS mask. The diverging light after this mask passes through a Wollaston prism, which separates the two polarization states of light. These two pupil images are recorded on a CRED-2 detector manufactured by First Light Imaging [REF].

The ZWFS installed at the Keck telescope uses a vector Zernike mask to impart different phase offsets to the two orthogonal polarizations of incident light [18]. This mask, shown in Figure 7, is made of a meta-surface material composed of nano-pillars to introduce a  $\pi/2$  and  $-\pi/2$  phase offset to orthogonal linear polarizations. Using the vector-ZWFS introduces diversity in the measurements, the two pupil images are used to increase the dynamic range with respect to the scalar-ZWFS. Reconstruction of the vector-ZWFS is performed by using an iterative non-linear algorithm which use a numerical model of the optical propagation trough the sensor along with the diversity produced by the dual measurements on each polarization.

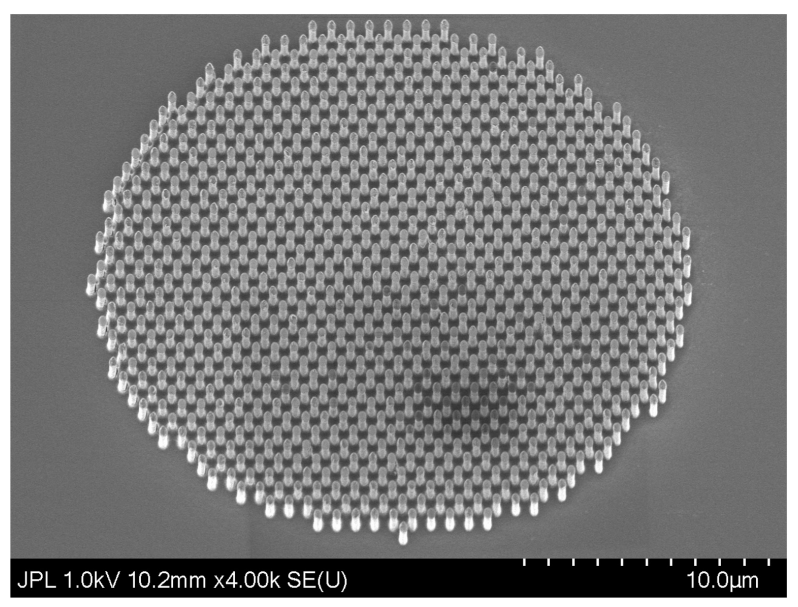


Figure 7. Shown is an scanning electron microscope (SEM) image of the vector ZWFS mask fabricated at JPL's Mircodevices Laboratory (MDL). The mask uses polarization effects to improve the dynamic range of the ZWFS while on sky.

### 3.1 Non-Common Path Aberrations Compensation

The main goal of the vector-ZWFS is to measure segment co-phasing errors, but it is also used as a calibration tool for NCPAs. The vector-ZWFS is routinely used as part of daytime calibrations to set up KPIC for night observations by correcting NCPAs from the SHWFS. This operation is run in closed loop with the Keck Xinetics DM. The PSF is centered on the vector-ZWFS dimple and NCPAs are measured by reconstructing the signals obtained using the CRED-2 to image the pupil plane. Reconstructed NCPAs are compensated by closing the loop, as shown in Figure 8, between the vector-ZWFS and the BMC kilo-DM, which is internal to the KPIC instrument. The corrections are mainly low order aberrations caused by NCPA between the SHWFS and KPIC optical paths, but higher spatial frequencies present most likely arise from the typical Keck AO calibrations. Some aberrations at the edge of the DM are left uncorrected by the closed loop, but they have very little impact on sky as the Keck telescope pupil is smaller than the DM. The final residual wavefront amplitude inside the Keck pupil footprint is estimated to be less than 30 nm rms after this calibration.

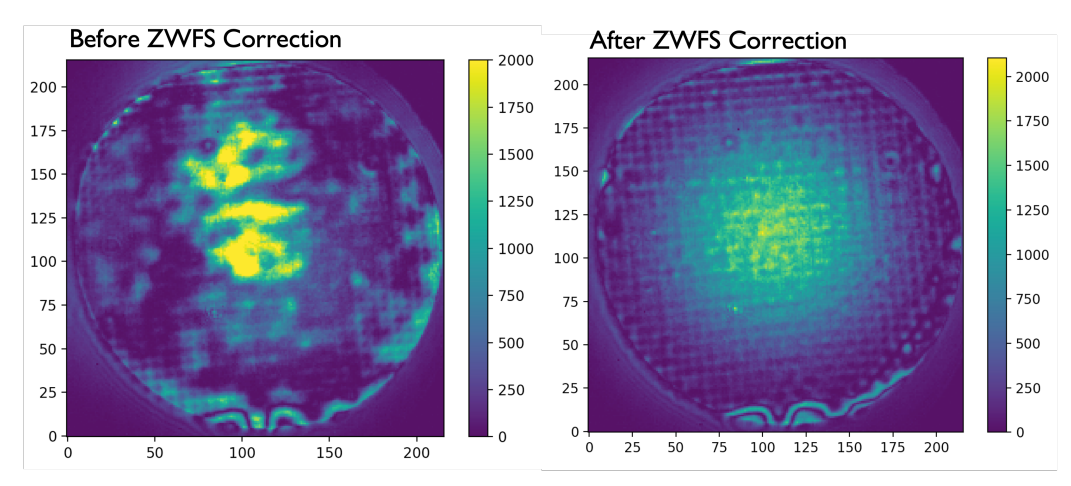


Figure 8. NCPAs compensation during daytime calibrations with vector-ZWFS. Shown is one of the pupil plane images when centered on the ZWFS mask, before and after closed loop with the internal KPIC DM.

# 3.2 On-Sky Primary Mirror Corrections

The goal of this demonstration is to sense and control the primary mirror segments in closed-loop in parallel with NIRC2 science observations. When the PyWFS is used the ZWFS receives up to 10% of the light in J and H-band, with 90% used for the PyWFS. The ZWFS can also be used in parallel with SHWFS observations, if observers are willing to sacrifice J and H-band light from their science. In this case the ZWFS will receive 100% of the light in J and H-band. The vector-ZWFS has been tested on-sky and shown to accurately measure primary mirror segment phasing errors. By averaging each image over 30 seconds, atmospheric turbulence residuals are decoupled from piston errors and the primary mirror is visible, as shown in Figure 9. From the two pupil images, the wavefront phase is reconstructed using an analytical model of the system and an iterative algorithm, following the method in Steeves et al. 2020 [16]. Individual segment pistons are extracted after removing the global tip-tilt and focus modes.

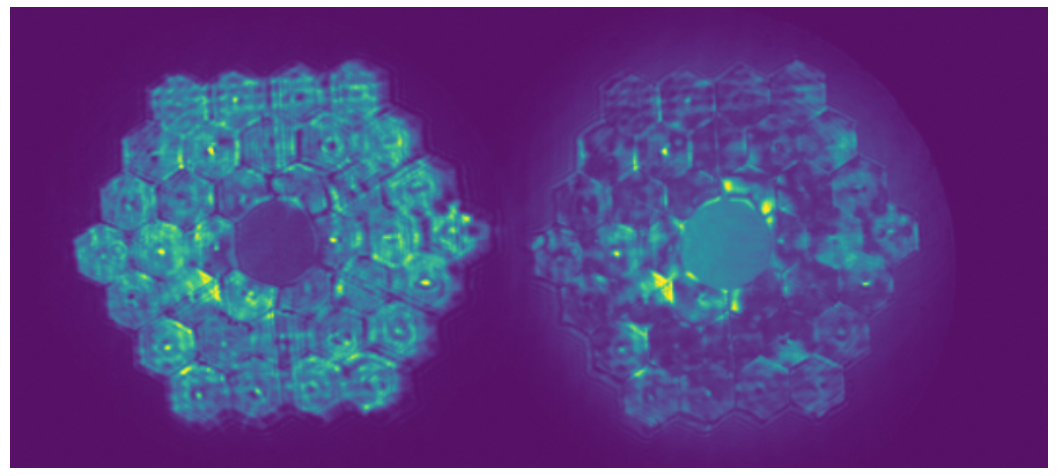


Figure 9. A 30-second averaged pupil image of the Keck primary mirror taken with the vector-ZWFS on January 9th, 2023 using a narrow band filter centered on 1550nm. The segment piston errors are reconstructed from these images.

To build an understanding of the sensitivity to primary mirror piston errors three segments were pistoned over a range of amplitudes (-400, -200, -100, -50, +50, +100, +200, and +400 nm in OPD). Their resulting piston values were measured with the vector-ZWFS, visualized in Figure 10. The three pistoned segments visually appeared brighter during the observation without any post-processing. Subtracting the nominal flat mirror image, the three segments stand out even more. While the phase is underestimated initially, the vector-ZWFS converges

on a solution quickly when run in closed loop.

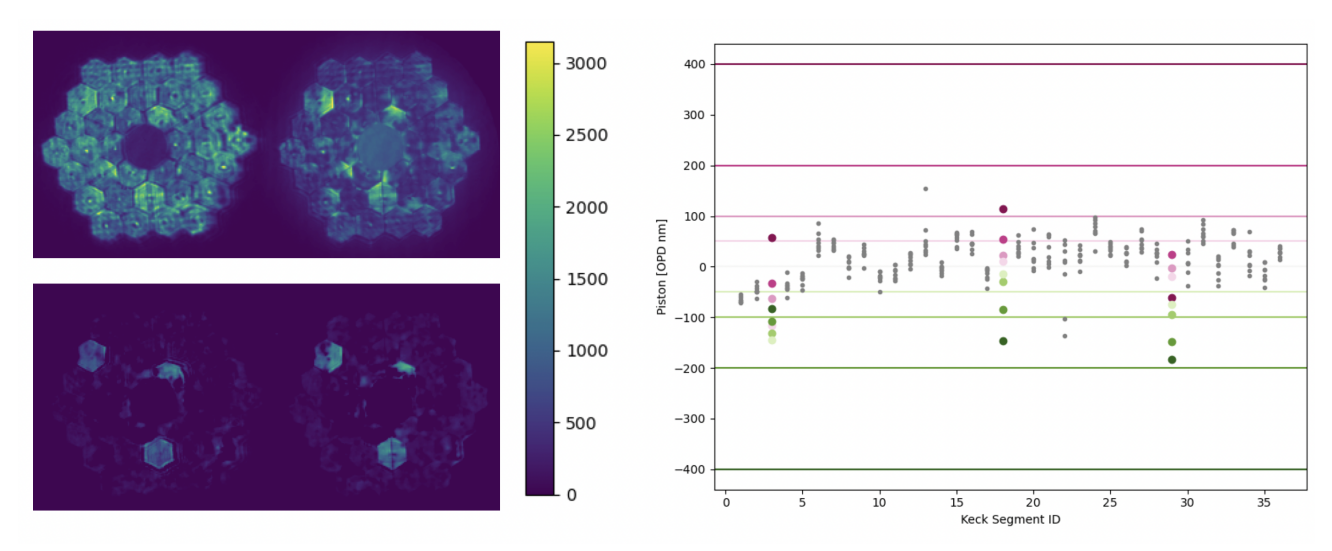


Figure 10. Top Left: The vector-ZWFS image after pistoning 3 segments of the Keck primary mirror while observing a bright star. Segments 3, 18, and 29 were pistoned by 200nm. Changes to the pupil plane were visible by eye during this test. Bottom Left: Shown is the difference between the above image and a pupil image using the nominal flat position of the segments. Right: Shown is a visualization of the reconstructed segment piston values (in OPD, nm) for each segment. Values are shown when pistoning segments 3, 18, and 29 by 400, 200, 100, and 50nm in each direction. The ZWFS routinely underestimates the piston errors, but converges quickly during multiple estiamtions.

#### 4. SPECKLE NULLING ON NIRC2

One of the challenges faced in direct imaging is the presence of speckle aberrations in the focal plane due to NCPAs. While differential imaging can remove such aberrations during post-processing, an optical-based approach is preferred. In post-processing, the intensity of the speckles can only be subtracted down to the photon noise limit. Instead, if the brightness of the speckle is reduced before detection, the associated noise can be reduced further. An optimal solution is to use images in the focal plane to sense these additional errors.

Multiple speckle nulling methods in the focal plane have been previously tested on the Keck telescope [2]. A simple approach involves destructive interference by adding a corresponding phase to the electric field to cancel an existing speckle, with a basic system model and calibration. The first step of this method is determining the electric field phase component. To do this, the deformable mirror is used to introduce a known perturbation in the focal plane. An opposing electric field is generated from this measurement and applied using the deformable mirror. A specific example of this is a speckle nulling method described in Traub & Oppenheimer 2010 [17].

# 4.1 Preliminary Results on NIRC2

The work on NIRC2 explores different algorithms based on phase shifting interferometry (PSI) techniques. The performance levels are compared to inform a facilitized speckle suppression pipeline algorithm. The algorithms all involve an iterative nulling loop with 4-, 3-, and 2-step PSI calculations. Varying the number of phase shifts induced on the reference beam and the difference between phase angles tests a balance of nulling depth and convergence time. Multiple trials for each algorithm conducted with a simulation of the Keck vortex coronagraph. The results concluded that 3 and 4-step PSI algorithms prove to be more effective at nulling despite the larger time to converge, shown in Figure 11. In cases where a faster readout time is preferred a 2-step algorithm may be used.

Currently these algorithms are in test on the Keck II AO bench to build a more robust calibration system by normalizing the speckle intensity with the satellite intensity, shown in Figure 12. In simulation this method works just as well without normalized speckle intensity. Once the system is stable enough, the speckle nulling

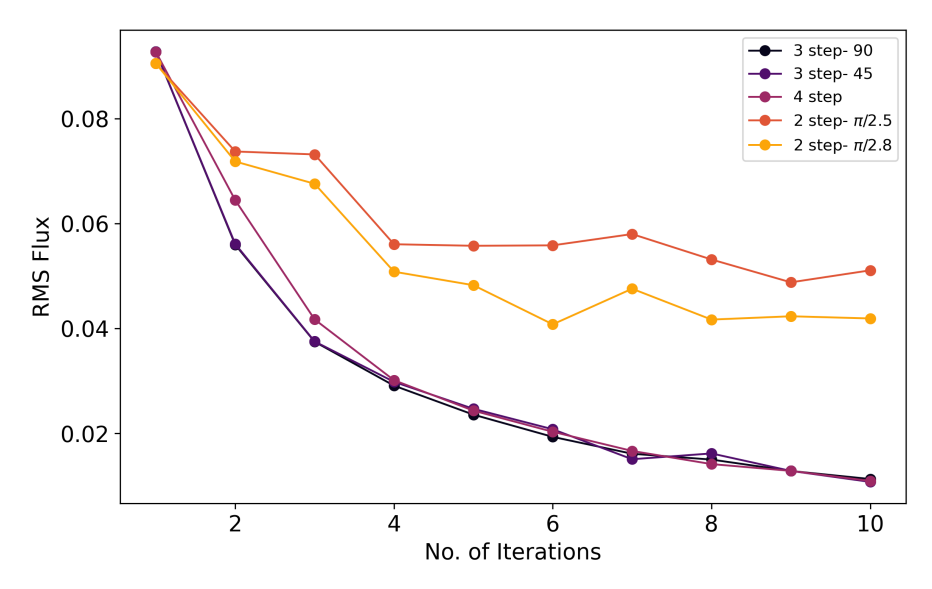


Figure 11. Simulated results testing the nulling depth of a 4-, 3-, and 2-step speckle nulling algorithm. As shown, the 4- and 3- algorithms converge to a deeper hole. The 2-step method converges in  $\frac{2}{3}$  the time as the 3-step and  $\frac{1}{2}$  since it requires less phase shifts.

code will be tested on the sky for stars with known companions. These on-sky tests will inform the operational tool which will be designed for this project.

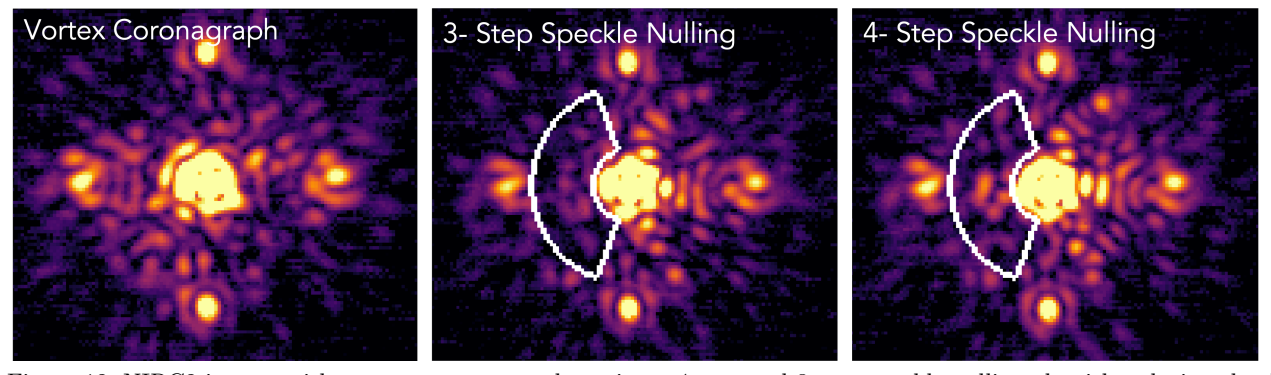


Figure 12. NIRC2 images with a vortex coronagraph testing a 4-step and 3-step speckle nulling algorithm during the day.

# 5. PREDICTIVE WAVEFRONT CONTROL

For high contrast imaging applications, AO systems are often also limited by bandwidth error. This error is introduced by time lag in the AO system, when the speed at which a correction is applied is slower than the speed at which the atmosphere is changing. The time lag of the Keck AO system, before the current real time controller upgrade, is roughly 1.5ms [4]. In coronagraphic images, any scattered light can impact the performance of the coronagraph. This is especially true for NIRC2, where the vortex corongraph induces phase variation to direct light. The wind-driven halo [3] is a feature which appears when using a coronagraph, where light is scattered into the dark region. This feature appears in the direction of the moving wind layers, as the correction is essentially blown into the past.

Empirical orthogonal functions (EOF) offers a solution, as a predictive wavefront control (pWFC) method that learns linear trends of the wavefront turbulence in time. The dominant feature expected is from the wind-driven atmospheric layers, however in practice EOF also predicts vibrations and other regular features. The EOF estimate is applied as a pseudo-open loop correction, running the AO loop with effectively no lag time by estimating where the atmosphere will be by the time the correction is applied. This has the potential to maximize sky coverage by allowing longer exposures for fainter guide stars. EOFs were first suggested in Guyon, 2017 [6], demonstrated on the Subaru telescope [7], applied in simulation as a post processing method using Keck telemetry [8, 5], and tested on-sky on the Keck II telescope [12].

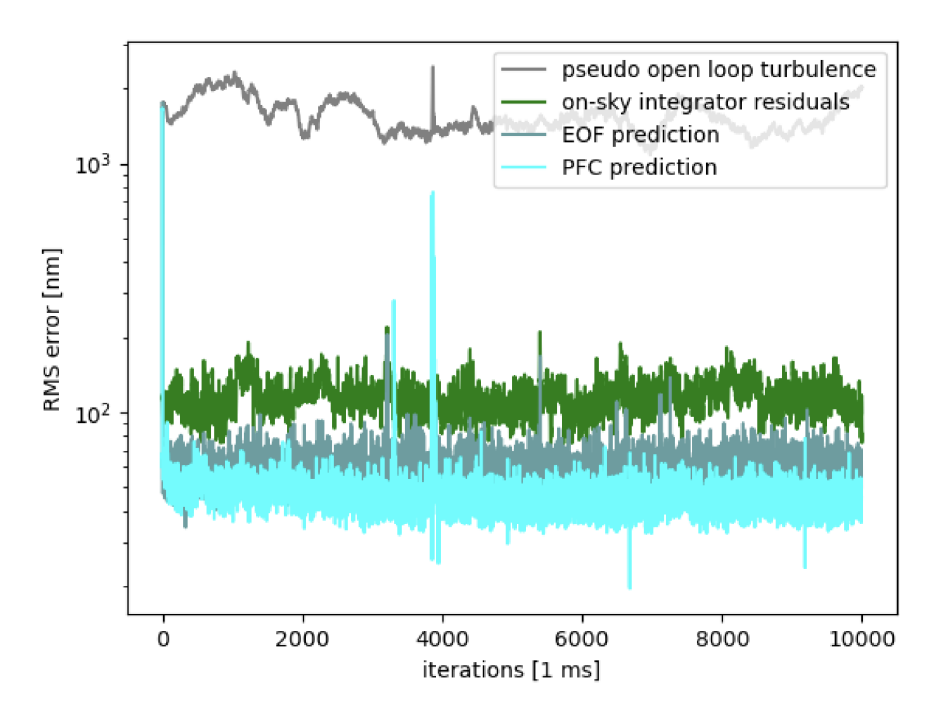


Figure 13. Root mean square error imparted on an image from different control methods, PFC in blue and EOF in blue-grey [5]. Pseudo open loop turbulence is reconstructed shown in grey. The integrator residuals seen by the WFS are in green.

Current efforts focus on 1) exploring the performance of EOF and other predictive methods on simulated Keck data and telemetry as a post processing method [5], 2) performing lab testing with the Santa Cruz Extreme AO Lab (SEAL) testbed, and 3) continuing on-sky testing on the Keck II telescope to better benchmark and stabilize the performance of EOF on NIRC2. The simulated results from [5], shown in Figure 13, apply predictive methods to Keck AO telemetry including the EOF method and Predictive Fourier control (PFC). Each method shows a decrease in RMS error, an overall improvement factor of 1.9 for EOF and 2.5 for PFC[13] over the current Keck II integrator residuals. The most current results from [12], shown in Figure 14, use an initial implementation of EOF on-sky for NIRC2 with a factor of 3 improvement in contrast over a classic integrator at 3-7  $\lambda$ /D, a 1.5 factor decrease in standard deviation during L band coronagraphic observations. A Strehl ratio increase was also shown from  $\sim 19\%$  with the integrator to  $\sim 23\%$  with EOF for observations with the narrowband Bracket  $\gamma$  filter.

# 6. CONCLUSION

The four high contrast imaging projects currently being developed into operational tools will improve the uncorrected AO errors currently limiting high contrast imaging through a simple, easy to operate, and robust interface. Fast and Furious has been demonstrated previous on-sky with promising results as a focal plane wavefront sensor. This motivated a push to make an operational tool using science images on NIRC2 to correct NCPAs missed during daytime calibrations. A ZWFS was installed as a part of a previous KPIC upgrade and has been used to image the piston offsets of segments on the Keck II primary mirror. This WFS has been demonstrated an ability to recover piston errors down to 50nm that the SHWFS is blind too. A speckle nulling and predictive wavefront control tool are also in development to improve extreme AO observations with a coronagraph. These projects benefit the high contrast observations at Keck Observatory and developing them into operational tools will make them available for more observers.

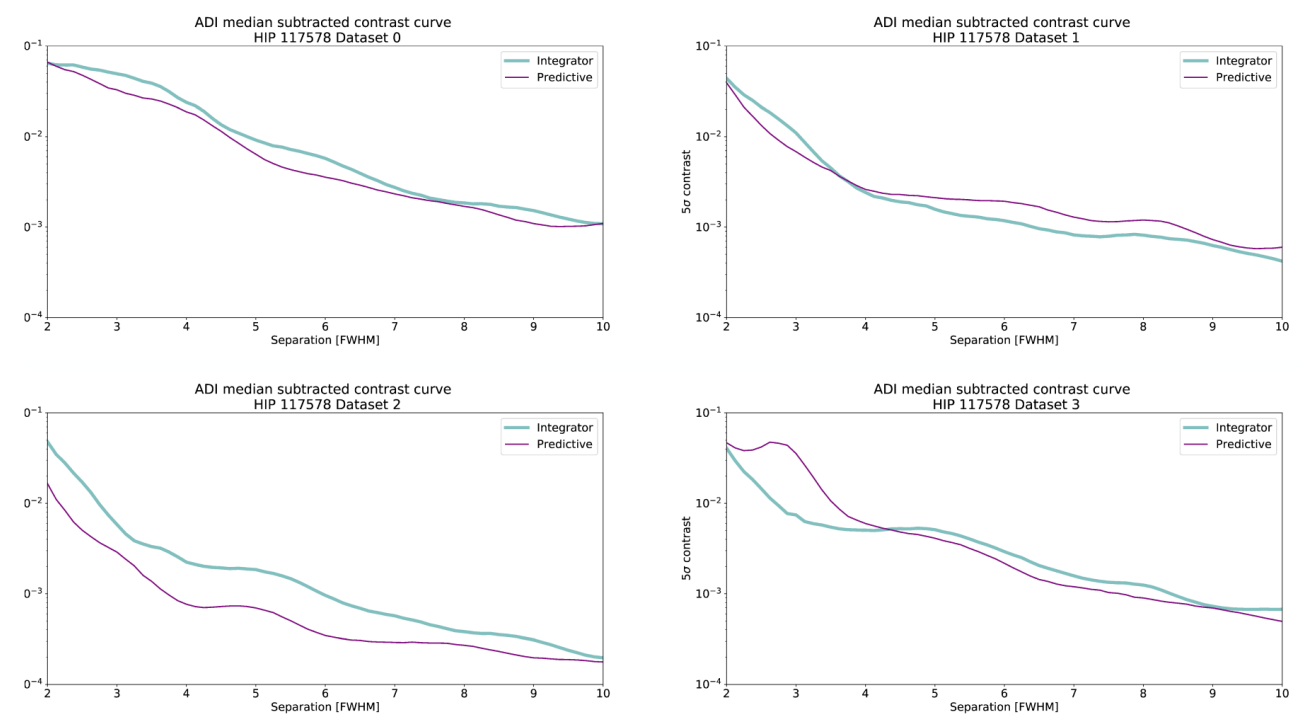


Figure 14. The impact of EOF on coronagraphic contrast is shown for L band observations with NIRC2 [12]. Filter parameters were changing during these runs, showing varied performance from the predictive method and motivating future work to optimize an EOF predictor on-sky.

#### ACKNOWLEDGMENTS

This work was funded by the Heising-Simons Foundation through a postdoctoral fellowships from Grant No. 2021-3193. Fast and Furious and Speckle Nulling work is supported by National Science Foundation Award No. 2009051. Zernike Wavefront Sensor and Predictive wavefront control work was supported by the Heising-Simons. The W. M. Keck Observatory is operated as a scientific partnership among the California Institute of Technology, the University of California, and the National Aeronautics and Space Administration. The Observatory was made possible by the generous financial support of the W. M. Keck Foundation. The authors wish to recognize and acknowledge the very significant cultural role and reverence that the summit of Maunakea has always had within the indigenous Hawaiian community. We are most fortunate to have the opportunity to conduct observations from this mountain.

# References

- [1] Steven P. Bos et al. "Fast" and Furious focal-plane wavefront sensing at W. M. Keck Observatory. 2021. DOI: 10.48550/ARXIV.2107.07601. URL: https://arxiv.org/abs/2107.07601.
- [2] Michael Bottom et al. "Speckle nulling wavefront control for Palomar and Keck". In: Adaptive Optics Systems V. Ed. by Enrico Marchetti, Laird M. Close, and Jean-Pierre Véran. Vol. 9909. International Society for Optics and Photonics. SPIE, 2016, p. 990955. DOI: 10.1117/12.2233025. URL: https://doi.org/10.1117/12.2233025.
- [3] F. Cantalloube et al. "Wind-driven halo in high-contrast images. I. Analysis of the focal-plane images of SPHERE". In: 638, A98 (June 2020), A98. DOI: 10.1051/0004-6361/201937397. arXiv: 2003.05794 [astro-ph.IM].

- [4] Sylvain Cetre et al. "A near-infrared pyramid wavefront sensor for Keck adaptive optics: real-time controller". In: Adaptive Optics Systems VI. Ed. by Laird M. Close, Laura Schreiber, and Dirk Schmidt. Vol. 10703. Society of Photo-Optical Instrumentation Engineers (SPIE) Conference Series. July 2018, 1070339, p. 1070339. DOI: 10.1117/12.2311781.
- [5] J. Fowler, M. A. M. Van Kooten, and R. Jensen-Clem. "Battle of the predictive wavefront controls: comparing data and model-driven predictive control for high contrast imaging". In: *Adaptive Optics Systems VIII*. Ed. by Laura Schreiber, Dirk Schmidt, and Elise Vernet. Vol. 12185. Society of Photo-Optical Instrumentation Engineers (SPIE) Conference Series. Aug. 2022, 1218582, p. 1218582. DOI: 10.1117/12.2629521. arXiv: 2208.00984 [astro-ph.EP].
- [6] Olivier Guyon and Jared Males. "Adaptive Optics Predictive Control with Empirical Orthogonal Functions (EOFs)". In: arXiv e-prints, arXiv:1707.00570 (July 2017), arXiv:1707.00570. DOI: 10.48550/arXiv.1707.00570. arXiv: 1707.00570 [astro-ph.IM].
- [7] Olivier Guyon et al. "The compute and control for adaptive optics (CACAO) real-time control software package". In: *Adaptive Optics Systems VI*. Ed. by Laird M. Close, Laura Schreiber, and Dirk Schmidt. Vol. 10703. Society of Photo-Optical Instrumentation Engineers (SPIE) Conference Series. July 2018, 107031E, 107031E. DOI: 10.1117/12.2314315.
- [8] Rebecca Jensen-Clem et al. "Demonstrating predictive wavefront control with the Keck II near-infrared pyramid wavefront sensor". In: Society of Photo-Optical Instrumentation Engineers (SPIE) Conference Series. Vol. 11117. Society of Photo-Optical Instrumentation Engineers (SPIE) Conference Series. Sept. 2019, 111170W, 111170W. DOI: 10.1117/12.2529687. arXiv: 1909.05302 [astro-ph.IM].
- [9] N. Jovanovic et al. "Enhanced high-dispersion coronagraphy with KPIC phase II: design, assembly and status of sub-modules". In: *Ground-based and Airborne Instrumentation for Astronomy VIII*. Ed. by Christopher J. Evans, Julia J. Bryant, and Kentaro Motohara. Vol. 11447. International Society for Optics and Photonics. SPIE, 2020, 114474U. DOI: 10.1117/12.2563107. URL: https://doi.org/10.1117/12.2563107.
- [10] Christoph U. Keller et al. "Extremely fast focal-plane wavefront sensing for extreme adaptive optics". In: SPIE Proceedings. Ed. by Brent L. Ellerbroek, Enrico Marchetti, and Jean-Pierre Véran. SPIE, Sept. 2012. DOI: 10.1117/12.926725. URL: https://doi.org/10.1117%2F12.926725.
- [11] Maaike A. M. van Kooten et al. "On-sky Reconstruction of Keck Primary Mirror Piston Offsets Using a Zernike Wavefront Sensor". In: *The Astrophysical Journal* 932.2 (June 2022), p. 109. DOI: 10.3847/1538-4357/ac6ba2. URL: https://doi.org/10.3847%5C%2F1538-4357%5C%2Fac6ba2.
- [12] Maaike A. M. van Kooten et al. Predictive wavefront control on Keck II adaptive optics bench: on-sky coronagraphic results. 2022. DOI: 10.48550/ARXIV.2205.14164. URL: https://arxiv.org/abs/2205.14164.
- [13] Lisa A. Poyneer, Bruce A. Macintosh, and Jean-Pierre Véran. "Fourier transform wavefront control with adaptive prediction of the atmosphere". In: *Journal of the Optical Society of America A* 24.9 (Jan. 2007), p. 2645. DOI: 10.1364/JOSAA.24.002645.
- [14] Sam Ragland and Luke Gers. "A phase retrieval technique to measure and correct residual segment piston errors of large aperture optical telescopes". In: *Ground-based and Airborne Telescopes IX*. Ed. by Heather K. Marshall, Jason Spyromilio, and Tomonori Usuda. Vol. 12182. International Society for Optics and Photonics. SPIE, 2022, p. 1218209. DOI: 10.1117/12.2630309. URL: https://doi.org/10.1117/12.2630309.
- [15] Sam Ragland et al. "Residual wavefront control of segmented mirror telescopes". In: Adaptive Optics Systems VIII. Ed. by Laura Schreiber, Dirk Schmidt, and Elise Vernet. Vol. 12185. International Society for Optics and Photonics. SPIE, 2022, 121850Y. DOI: 10.1117/12.2630269. URL: https://doi.org/10.1117/12.2630269.
- [16] John Steeves et al. "Picometer wavefront sensing using the phase-contrast technique". In: Optica 7.10 (Oct. 2020), pp. 1267–1274. DOI: 10.1364/OPTICA.398768. URL: https://opg.optica.org/optica/abstract.cfm?URI=optica-7-10-1267.
- [17] W. A. Traub and B. R. Oppenheimer. "Direct Imaging of Exoplanets". In: *Exoplanets*. Ed. by S. Seager. 2010, pp. 111–156.

[18] J. Kent Wallace et al. "Architecting, Implementing and Observing with a Metasurface vector Zernike wavefront sensor on the Keck Telescope". In: Adaptive Optics for Extremely Large Telescopes. 2023. URL: https://ao4elt7.sciencesconf.org/458799.